# Dual-Frequency 2D IR on Interaction of Weak and Strong IR Modes

### Dmitry V. Kurochkin, Sri Ram G. Naraharisetty, and Igor V. Rubtsov*

*Department of Chemistry, Tulane University, New Orleans, Louisiana 70118*

*Received: October 11, 2005; In Final Form: October 27, 2005*

Dual-frequency 2D IR heterodyne photon-echo spectroscopy of C≡N and C=O stretching vibrational modes in 2-cyanocoumarin is reported. We have shown that the interaction among these modes provides convenient and useful structural constraints for molecules. Implementation of two pulse sequences, 4, 4, and 6 $\mu$m and 6, 6, and 4 $\mu$m, allowed the clear determination of contributions caused by vibrational relaxation. Positive correlation between C≡N and C=O frequency distributions was observed in 2-cyanocoumarin. Because C≡N modes are highly localized and have frequencies in a spectral region with minimal water absorption, the C≡N/C=O interactions have a strong potential for use as structural reporters in proteins. In addition to CN/CO peaks, the cross-peaks responsible for the C≡N/C=C interaction are also observed in the 2D IR spectra, where C=C is a coumarin ring stretching mode. We have demonstrated that 2D IR spectroscopy can utilize interactions of strong IR modes with weak local modes as structural reporters.

## Introduction

The remarkable potential of 2D IR spectroscopy for determining the structure of molecules in solution has recently been demonstrated.[1−3] 2D IR experiments on C=O stretching modes (6 $\mu$m) in peptides,[1,2,4−7] carbonyl complexes,[8] and liquids[9] have been reported. The 3 $\mu$m spectral region has also been explored, including studies on the OH stretch in water[10−12] and in alcohols,[13] and the NH stretch in peptides.[14−16] Measurements in the 5 $\mu$m spectral region include experiments on OD and ND stretching modes, C≡N mode in complexes, and SCN⁻ ions.[15,17−21] Chemical exchange 2D IR spectroscopy has been demonstrated.[22] The accuracy and specificity of the structural constraints obtained by 2D IR depend strongly on how localized the reporting modes are. It has been known for decades that strongly interacting CO modes in proteins cannot be treated as isolated modes;[23,24] their interaction is strong enough to make them delocalized. Therefore, CO-mode interactions in protein can generally reveal structural information regarding secondary structure ($\alpha$-helix, $\beta$-sheet, and $\gamma$-turns). To access atom-sensitive structural constraints, several isotope substitution schemes have been implemented in 2D IR, including $^{13}$C, $^{18}$O, and deuterium labeling.[25,26] Dual-frequency heterodyne-detection 2D IR spectroscopy been developed, allowing the observation of interactions among modes from different spectral regions.[14,27−29] Frequency correlations of NH and CO groups forming a hydrogen bond have also recently been reported.[15]

The stretching mode of a cyano group, with the absorption peak at ca. 2240 cm⁻¹, is conveniently located in the featureless region of water absorption and has been used as a label in linear-IR spectroscopy.[30] The properties of the CN stretch mode in metal carbonyls have been studied by 2D IR in the 5 $\mu$m spectral region.[31] The mode is highly localized and has an extinction coefficient of ca. 30−100 M⁻¹ cm⁻¹ in different structures.[20]

## SCHEME 1
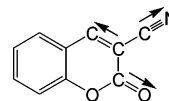
In this report, we investigated the interaction of CN and CO stretching modes in 2-cyanocoumarin via dual-frequency heterodyne photon-echo 2D IR experiments. We have chosen 2-cyanocoumarin because it has both cyano and carbonyl groups attached in adjacent positions on the coumarin ring and a rigid structure. Because these experiments are the first probing CN/CO interactions, we began the study with a sample that has a small separation distance between the groups in question; the center-to-center distance between CN and CO groups in 2-cyanocoumarin is ca. 3.1 Å. Two pulse sequences have been used that excite either CN or CO modes with the first two pulses. The correlations in CO and CN frequency distributions were measured.

## Experimental Methods

**Sample and Linear-IR Spectra.** A solution of 89 mM 2-cyanocoumarin (Scheme 1) in methylene chloride was used in the 2D IR experiments. Three vibrational modes were involved in this study: −C≡N (2240 cm⁻¹), >C=O (1744 cm⁻¹), and −C=C− (1608 cm⁻¹). The directions of their transition moments are shown in Scheme 1. The optical density of the sample, placed in a 50 $\mu$m path length CaF$_2$ cell, was 0.34 at 1744 cm⁻¹, 0.023 at 2240 cm⁻¹, and 0.15 at 1608 cm⁻¹. The ratio of integrated CO to CN peaks is 24 ± 2. The value of the CN transition dipole in 2-cyanocoumarin is measured at 0.07 D, which is ca. 5.6 times smaller than that of the CO mode (0.39 D).

**Dual-Frequency Heterodyned 2D IR.** Laser pulses at 806 nm, 44 fs in duration, produced by a Ti:sapphire-oscillator/

---

**10800** *J. Phys. Chem. A, Vol. 109, No. 48, 2005*

Letters



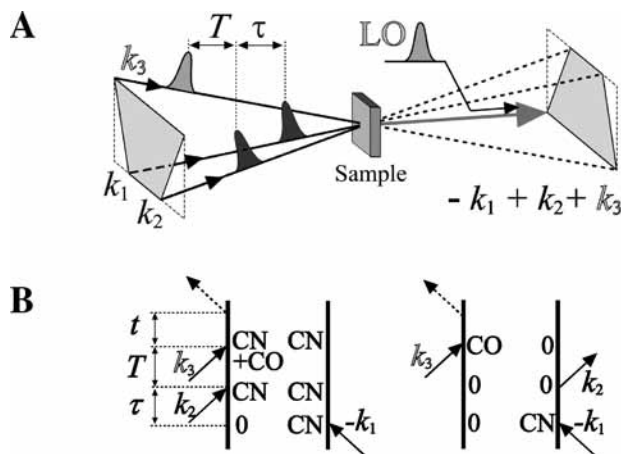**Figure 1.** (A) IR pulse geometry for the dual-frequency experiments. $k_1$ and $k_2$ pulses are centered at 4 μm, and $k_3$ and the local oscillator (LO) pulses are centered at 6 μm. A third-order signal, picked up from the phase matching direction $(-k_1 + k_2 + k_3)$, is mixed with the LO. (B) Double-sided Feynman diagrams responsible for the CN/CO cross-peaks in the rephasing experiments.

regenerative-amplifier tandem (Vitesse/USP-Legend, Coherent) were used to generate two sets of near-IR signal and idler pulses in two in-house built optical parametric amplifiers (OPA).[32] Each signal-idler pair was used to produce mid-IR pulses via difference frequency generation in a 1.5 mm thick AgGaS$_2$ crystal. The pulses at 4 μm (2 μJ/pulse, 90 fs) and 6 μm (1.4 μJ/pulse, 90 fs) were used in the experiments reported. Each mid-IR beam was split into two equal parts; three pulses were focused onto the sample and the fourth was used as a local oscillator (LO). A third-order signal generated in the sample was picked at the phase matching direction $(-k_1 + k_2 + k_3)$, mixed with the LO, delayed by a time $t$, and detected by an MCT detector (Infrared Associates). The spectral width of the pulses was $176 \pm 5$ cm$^{-1}$.

Most of the experiments were performed with a 4, 4, and 6 μm pulse sequence (Figure 1), so that the $k_1$ and $k_2$ beams 4 μm were tuned to match the CN absorption, whereas the $k_3$ and LO beams at 6 μm were tuned to match the CO peak. Two-dimensional $(\tau, t)$ spectra were recorded and double Fourier transformed to obtain $(\omega_\tau, \omega_t)$ spectra. Within the 4, 4, 6 μm sequence, rephasing experiments were collected when the $k_1$ beam arrived first and the $k_2$ beam arrived second; for nonrephasing spectra, the order of the first two beams was reversed. The rephasing pathways describing the cross-peaks are shown in Figure 1B. The geometry of the beams interacting with the sample is shown in Figure 1A. Phase-matching conditions for the dual-frequency experiments lead to a trapezoid pattern in the plane crossing the beams behind the sample cell so that the beams with higher frequency hit the shorter-base corners (Figure 1A). Only pairwise phase locking is required for the sequences used in this study;[15] the $k_1$ and $k_3$ pulses were possibly not phase locked.

An alternative 6, 6, 4 μm pulse sequence was also used in the 2D IR experiments. Rephasing and nonrephasing experiments were performed by interchanging the order of the first and second pulses. The beam geometry had to be fully reversed. All 2D spectra presented in this paper were recorded at room temperature with a $(zzzz)$ polarization conditions.

Infrared pump−probe measurements at 4 μm were performed to investigate the excited-state population dynamics of the CN mode in cyanocoumarin. The probe beam passed the sample was dispersed in a monochromator (TRIAX-190, JY) and recorded by an MCT detector. The bleach decay at 2240 cm$^{-1}$

(data not shown) was fitted well with a sum of two exponents: $1.7 \pm 0.1$ ps ($81 \pm 1\%$) and $19 \pm 2$ ps ($19 \pm 1\%$).

## Results and Discussion

Rephasing and nonrephasing experiments were performed using the 4, 4, 6 μm pulse sequence. Because the absolute phases of the IR pulses was not known, the phase in the complex 2D spectra had to be corrected. One way to tune the phase was to match the pump−probe spectra and a projection of the real part of the 2D spectrum.[33] Because the cross-peak signal in the dual-frequency pump/probe measurement was too small to be measured, the phases of the spectra were adjusted by aiming for the ratio of the bleach $(\omega_1, \omega_2)$ to the absorption $(\omega_1 - \Delta_{12}, \omega_2)$ peak amplitudes to be 1.1. This value, although arbitrary, reflected the lifetime shortening in the combination state with respect to the singly excited-state. Because the modes in question were not strongly interacting, the difference between the bleach and absorption amplitudes was not expected to be large. This pattern was observed in previous experiments as well.[27,34] Variation of this value in the 1.05−1.2 range did not influence the modeling parameters. The absorptive spectrum obtained by summing the real parts of the rephasing and nonrephasing spectra measured at $T = 670$ fs is shown in Figure 2A. Reasonably strong cross-peaks at $(\omega_{CO}, \omega_{CN})$ and $(\omega_{CO} - \Delta_{CO,CN}, \omega_{CN})$, deriving from CN and CO-mode interaction, dominate the spectrum. The peaks have a clear tilt in the diagonal direction with $\tan(\alpha) = 0.11 \pm 0.03$ (Figure 1A). This tilt originated from a correlation of the frequency distributions of the interacting modes.[14,27,33] The tilt toward the diagonal indicated a positive correlation factor for the CN/CO frequency distributions.[35] Simultaneous modeling of the linear and 2D IR spectra (Figure 2B) resulted in the correlation factor of $0.55 \pm 0.2$. Preliminary semiempirical calculations with normal-mode analysis showed that the frequencies of the CN and CO modes changed concomitantly when the molecule was transferred from vacuum to water, indicating that the correlation factor was positive. Interestingly, additional peaks were observed in the 2D IR spectrum, including cross-peaks at ca. (1608, 2240 cm$^{-1}$) and diagonal CO stretch peaks at ca. (1740, 1740 cm$^{-1}$).

It was surprising to observe the CO diagonal peaks in the 2D spectra optimized for observing the CN/CO cross-peaks. The intensity of the $k_1$ and $k_2$ pulses centered at 2240 cm$^{-1}$ was very small at 1740 cm$^{-1}$, but not zero. For example, for the spectrum in Figure 2A the ratio $(\xi)$ of the IR intensity of the $k_1$ and $k_2$ pulses at 1740 cm$^{-1}$ with respect to the maximum intensity at ca. 2240 cm$^{-1}$ was as small as $2.1 \times 10^{-3}$.[36] The electric field emitted by the sample is proportional to the product of all three electric fields, $E_1$, $E_2$, and $E_3$, interacting with the sample.[3] The intensity drop by $\xi$ corresponded to a decrease in the electric-field amplitude by a $\sqrt{\xi}$ factor; the product of $E_1$ and $E_2$ recovered the $\xi$ factor for the echo-signal suppression. The diagonal peaks would be ca. 500 times stronger if the same intensity $k_1$ and $k_2$ spectra were shifted to 1740 cm$^{-1}$. A difference in the CO and CN transition moments was responsible for a factor of 24. Another factor of ca. 20 came from the difference in the CO diagonal ($\sim$14 cm$^{-1}$) and CN/CO off-diagonal anharmonicities. The value of the off-diagonal anharmonicity obtained via modeling was $1.7 \pm 1$ cm$^{-1}$.

The normal-mode analysis revealed that the mode at 1608 cm$^{-1}$ was the C=C stretching mode of the coumarin ring (Scheme 1). Observation of the cross-peaks at ca. (1608, 2240 cm$^{-1}$) was possible because the light intensity of the $k_3$ beam, centered at ca. 1730 cm$^{-1}$, was nonzero at 1608 cm$^{-1}$. In fact it was about 5 times smaller than the value at the maximum,

Letters

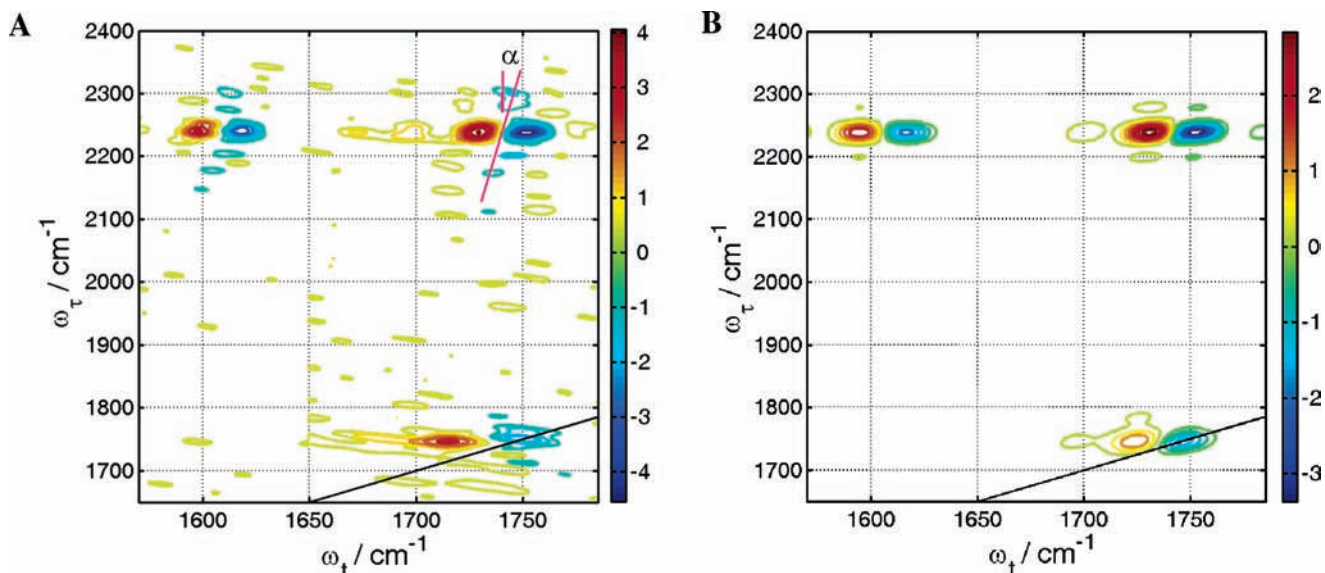*J. Phys. Chem. A, Vol. 109, No. 48, 2005* **10801**



**Figure 2.** (A) Dual-frequency 2D IR absorptive spectrum of 2-cyanocoumarin in methylene chloride at $T = 670$ fs. The intensity in the $k_1$ and $k_2$ pulses at 1740 cm$^{-1}$ was $2.1 \times 10^{-3}$ from the intensity at its maximum at ca. 2240 cm$^{-1}$. (B) Modeled spectrum calculated with the off-diagonal anharmonicities for CN/CO and CN/CC modes of 2.0 and 16 cm$^{-1}$, respectively, and correlation factors of 0.55 and 0.2, respectively. Note that the CN/CC peaks shape is not sensitive to the presence of the frequency correlations due to a small inhomogeneity of the C=C mode.
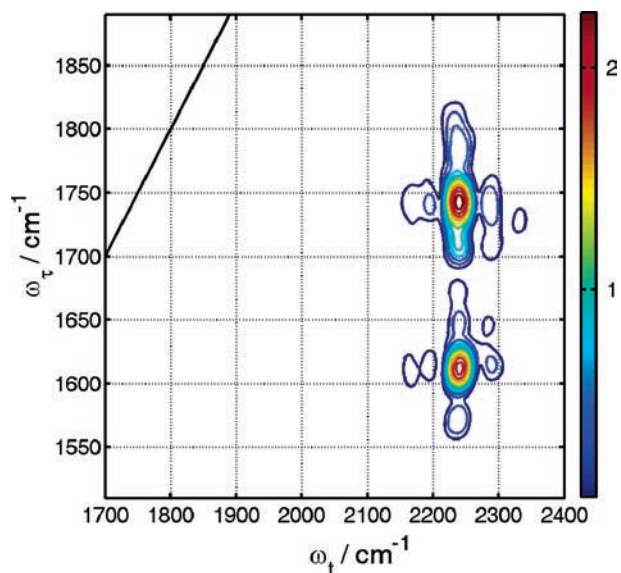


**Figure 3.** Absolute-value 6, 6, and 4 $\mu$m 2D IR rephasing spectrum of 2-cyanocoumarin at $T = 1$ ps. Diagonal CO peak cannot be seen because the pulse spectra are well separated.

significantly decreasing the amplitude of the CN/CC cross-peaks. The large value of the CN/CC off-diagonal anharmonicity, 12−20 cm$^{-1}$, obtained from the modeling, derived from a close proximity of these modes. The tilt of the CN/CC cross-peaks was not prominent due to the low inhomogeneity of the C=C mode.

It is known that vibrational relaxation affects the cross-peak shapes.[34] In our experiments, the CO mode can be populated via vibrational relaxation from the originally excited CN mode, which has higher energy. Following the relaxation, the character of the CO/CN cross-peak would change to diagonal CO/CO character hiding the CN/CO coupling information. To evaluate vibrational relaxation contributions, the experiments with the reversed pulse sequence, 6, 6, and 4 $\mu$m, were performed. Clear cross-peaks, similar to those in Figure 2A were observed, (Figure 3) confirming that direct CN/CO coupling was indeed observed. Vibrational relaxation dynamics will be described elsewhere.

The strategy employed here differs from previous approaches in its use of a weak local IR reporter. There are several advantages of using weak IR reporters, such as C≡N, in 2D IR. If the mode is weak and frequency separated from the other modes of the molecule, it will likely be a localized mode. Interactions of several weak modes with each other are too small to overcome the frequency separations introduced by the inhomogeneous broadening. Such modes are in the weak interaction limit when the frequencies of vibrational modes are determined by local environment rather than by the mode−mode interaction. Note that the weak interaction limit holds in 2D NMR spectroscopy. It is convenient to obtain structural parameters from the interaction of weak IR modes, such as CN, with strong modes, such as CO. Although CO modes in proteins are delocalized, it will be possible to obtain bond-sensitive structural constraints because the cross-peak amplitude in 2D spectra sharply depends on the distance between interacting groups (as $1/R^6$). Therefore, the interaction with the closest CO group will dominate the 2D spectrum. Current sensitivity of our 2D IR setup would allow detection of the interaction between CN and CO modes separated by up to 4.5 Å. With further improvements in the IR laser power and laser stability, the distances up to 6−7 Å are expected to be accessible by using this interaction. These experiments create the prospects of using weak IR modes as structural reporters. Additionally, the convenient spectral region of the CN mode makes these findings of even greater potential use.

**Supporting Information Available:** Details regarding experimental design and data treatment, as well as additional 2R spectrum. This material is available free of charge via the Internet at http://pubs.acs.org.

**10802** *J. Phys. Chem. A, Vol. 109, No. 48, 2005*

Letters

### References and Notes

(1) Hamm, P.; Lim, M.; Hochstrasser, R. M. *J. Phys. Chem. B* **1998**, *102*, 6123.

(2) Asplund, M. C.; Zanni, M. T.; Hochstrasser, R. M. *Proc. Natl. Acad. Sci. U.S.A.* **2000**, *97*, 8219.

(3) Mukamel, S. *Principles of Nonlinear Spectroscopy*; Oxford University Press: New York, 1995.

(4) Zanni, M. T.; Asplund, M. C.; Hochstrasser, R. M. *J. Chem. Phys.* **2001**, *114*, 4579.

(5) Hamm, P.; Lim, M.; DeGrado, W. F.; Hochstrasser, R. M. *Proc. Natl. Acad. Sci. U.S.A.* **1999**, *96*, 2036.

(6) Volkov, V.; Hamm, P. *Biophys. J.* **2004**, *87*, 4213.

(7) Mukherjee, P.; Krummel, A. T.; Fulmer, E. C.; Kass, I.; Arkin, I. T.; Zanni, M. T. *J. Chem. Phys.* **2004**, *120*, 10215.

(8) Golonzka, O.; Khalil, M.; Demirdoven, N.; Tokmakoff, A. *J. Chem. Phys.* **2001**, *115*, 10814.

(9) Ge, N.-H.; Hochstrasser, R. M. *Tr. Opt. Photon.* **2002**, *72*, 255.

(10) Eaves, J. D.; Loparo, J. J.; Fecko, C. J.; Roberts, S. T.; Tokmakoff, A.; Geissler, P. L. *Proc. Natl. Acad. Sci. U.S.A.* **2005**, *102*, 13019.

(11) Nibbering, E. T. J.; Elsaesser, T. *Chem. Rev.* **2004**, *104*, 1887.

(12) Corcelli, S. A.; Lawrence, C. P.; Asbury, J. B.; Steinel, T.; Fayer, M. D.; Skinner, J. L. *J. Chem. Phys.* **2004**, *121*, 8897.

(13) Gaffney, K. J.; Piletic, I. R.; Fayer, M. D. *J. Phys. Chem. A* **2002**, *106*, 9428.

(14) Rubtsov, I. V.; Wang, J.; Hochstrasser, R. M. *J. Chem. Phys.* **2003**, *118*, 7733.

(15) Rubtsov, I. V.; Kumar, K.; Hochstrasser, R. M. *Chem. Phys. Lett.* **2005**, *402*, 439.

(16) Park, J.; Ha, J.-H.; Hochstrasser, R. M. *J. Chem. Phys.* **2004**, *121*, 7281.

(17) Khalil, M.; Demirdoven, N.; Tokmakoff, A. *J. Chem. Phys.* **2004**, *121*, 362.

(18) Ohta, K.; Maekawa, H.; Tominaga, K. *Chem. Phys. Lett.* **2004**, *386*, 32.

(19) Ohta, K.; Maekawa, H.; Saito, S.; Tominaga, K. *J. Phys. Chem. A* **2003**, *107*, 5643.

(20) Helbing, J.; Bonacina, L.; Pietri, R.; Bredenbeck, J.; Hamm, P.; van Mourik, F.; Chaussard, F.; Gonzalez-Gonzalez, A.; Chergui, M.; Ramos-Alvarez, C.; Ruiz, C.; Lopez-Garriga, J. *Biophys. J.* **2004**, *87*, 1881.

(21) Asbury, J. B.; Steinel, T.; Kwak, K.; Corcelli, S. A.; Lawrence, C. P.; Skinner, J. L.; Fayer, M. D. *J. Chem. Phys.* **2004**, *121*, 12431.

(22) Kim, Y. S.; Hochstrasser, R. M. *Proc. Natl. Acad. Sci. U.S.A.* **2005**, *102*, 11185.

(23) Abbott, N. B.; Elloit, A. *Proc. R. Soc. A* **1956**, *234*, 247.

(24) Torii, H.; Tasumi, M. *J. Chem. Phys.* **1992**, *96*, 3379.

(25) Paul, C.; Wang, J.; Wimley, W. C.; Hochstrasser, R. M.; Axelsen, P. H. *J. Am. Chem. Soc.* **2004**, *126*, 5843.

(26) Fang, C.; Hochstrasser, R. M. *J. Phys. Chem. B* **2005**, *109*, 18652.

(27) Rubtsov, I. V.; Wang, J.; Hochstrasser, R. M. *Proc. Natl. Acad. Sci. U.S.A.* **2003**, *100*, 5601.

(28) Rubtsov, I. V.; Wang, J.; Hochstrasser, R. M. *J. Phys. Chem. A* **2003**, *107*, 3384.

(29) Scheurer, C.; Mukamel, S. *J. Chem. Phys.* **2002**, *116*, 6803.

(30) Getahun, Z.; Huang, C.-Y.; Wang, T.; De Leon, B.; DeGrado, W. F.; Gai, F. *J. Am. Chem. Soc.* **2003**, *125*, 405.

(31) Ohta, K.; Maekawa, H.; Tominaga, K. *J. Phys. Chem. A* **2004**, *108*, 1333.

(32) Details of the experimental setup will be reported in a following publication.

(33) Ge, N.-H.; Zanni, M. T.; Hochstrasser, R. M. *J. Phys. Chem. A* **2002**, *106*, 962.

(34) Rubtsov, I. V.; Hochstrasser, R. M. *J. Phys. Chem. B* **2002**, *106*, 9165.

(35) A correlation factor for static distributions is given by $f_{CN/CO} = \langle \delta\omega_{CN}(t)\, \delta\omega_{CO}(0)\rangle/(\sigma_{CN}\sigma_{CO})$, where $\delta\omega_A(t)$ is the frequency deviation from the mean value of the frequency distribution $\omega_A$ at time $t$.

(36) IR spectra were corrected for differences in monochromator dispersion at different wavelengths.